NOTES AND CORRESPONDENCE

Timing of El Niño–Related Warming and Indian Summer Monsoon Rainfall

CHIE IHARA, YOCHANAN KUSHNIR, MARK A. CANE, AND ALEXEY KAPLAN

Lamont-Doherty Earth Observatory, Columbia University, Palisades, New York

(Manuscript received 2 April 2007, in final form 17 October 2007)

ABSTRACT

The relationship between all-India summer monsoon rainfall (ISMR) and the timing of (El Niño–Southern Oscillation) ENSO-related warming/cooling is investigated, using observational data during the period from 1881 to 1998. The analysis of the evolutions of Indo-Pacific sea surface temperature (SST) anomalies suggests that when ISMR is not below normal despite the co-occurrence of an El Niño event, warming over the eastern equatorial Pacific starts from boreal winter and evolves early so that the western-central Pacific and Indian Ocean are warmer than normal during the summer monsoon season. In contrast, when the more usual El Niño–dry ISMR relationship holds, the eastern equatorial Pacific starts warming rapidly only about a season before the reference summer so that the western-central Pacific and Indian Oceans remain cold during the monsoon season.

1. Introduction

The all-India summer monsoon rainfall (ISMR; Sontakke et al. 1993), is defined as the total summer monsoon season (June–September) rainfall averaged over all of India. The El Niño–Southern Oscillation (ENSO) phenomenon is considered the most important external influence on ISMR since Walker found the connection between them in the early twentieth century. The monsoon season equatorial Pacific SST anomalies are negatively correlated with ISMR (Rasmusson and Carpenter 1983; Ropelewski and Halpert 1987). However, occasionally normal and above-normal ISMR occurs during the El Niño events of the monsoon season. Some studies claimed that in addition to the SST pattern related to "canonical" El Niño, the anomalous Indo or Pacific SST patterns during the monsoon season could be one of the determinants in explaining these unusual events (Ashok et al. 2004; Krishna Kumar et al. 2006). However, the seasonal evolution of SST anomalies over the Indo-Pacific regions should be considered, since both the ENSO cycle and the monsoon are seasonally phase locked. The canonical El Niño cycle begins with the evolution of the anomaly in the late spring followed by intensification throughout the summer to reach peak amplitude at the end of the year (Rasmusson and Carpenter 1982). This El Niño evolution pattern, however, is by no means invariable. An El Niño event can begin to develop in the winter and last through the following summer. The Indian Ocean SSTs are largely influenced by El Niño evolution; basin-scale warming is observed 3–6 months after the occurrence of El Niño events as reviewed by Alexander et al. (2002) and this can exert local influence on the monsoon. We therefore hypothesize that the atypical timing of warming over the equatorial eastern Pacific can impact the El Niño–monsoon relationship either directly, or indirectly through the feedbacks of El Niño–induced SST anomalies over the Indian monsoon region.

In this paper the link between the interannual variability of ISMR and time evolutions of Indo-Pacific SST anomalies is examined to address this issue using observational datasets from 1881 to 1998. We examine such long data in order to gain robust statistics. Data used in this study are described in section 2. Seasonal SST anomalies over the tropical Indo-Pacific Oceans when the ENSO–monsoon relationship breaks down are examined in section 3. In section 4, the evolutions of

Corresponding author address: Chie Ihara, Lamont-Doherty Earth Observatory, Columbia University, 61 Route 9W, Palisades, NY 10964-8000.
E-mail: cihara@ldeo.columbia.edu

DOI: 10.1175/2007JCLI1979.1

monthly ENSO and Indo-Pacific Ocean SST indices are shown. Section 5 is devoted to a summary and discussion.

2. Data descriptions

ISMR reconstructions based on station rainfall observations over India are obtained from Sontakke et al. (1993), and monthly gridded SST anomalies are obtained from Kaplan et al. (2003). Data prior to 1880 are not included in our analysis to avoid the large uncertainties of SST anomaly data in this early period (Kaplan et al. 1998). It is well known that Niño-3 index (i.e., SST anomalies averaged between 5°N–5°S and 90°–150°W) and Niño-3.4 index (i.e., SST anomalies averaged between 5°N–5°S and 120°–170°W) are more strongly correlated with ISMR than SST anomalies in closer regions. The correlation coefficient between ISMR and the June–September Niño-3 (Niño-3.4) during the years between 1881 and 1998 is −0.57 (−0.59). A scatterplot between ISMR and the June–September Niño-3 shows two extreme outliers; 1983, a rapidly decaying El Niño year having above-normal ISMR, and 1997, an extremely strong El Niño year having normal ISMR. Excluding these two years improves the correlation between ISMR and the June–September Niño-3 to −0.65. There are no extreme outliers in the scatterplot of ISMR and the June–September Niño-3.4.

El Niño years in our study are the years in which the monsoon season Niño-3 values between 1881 and 1998 fall in the upper 33% of the distribution (hereafter we call these 39 events "El Niño–3m"). La Niña years are those falling in the lower 33% ("La Niña–3m"). El Niño–3.4m/La Niña–3.4m are defined analogously, measuring the ENSO phase of the reference summer by Niño-3.4. El Niño–3.4m is almost equivalent to El Niño–3m in the earlier period analyzed, but El Niño–3.4m includes four successive years in the 1990s, from 1991 to 1994, as the discrepancy between these indices during this period is discussed in Weng et al. (2007) and Ashok et al. (2007). To avoid the effects of the long-lasting El Niños on our analysis, and to measure ENSO events by an index that shows a higher connection to ISMR variability, we mainly use Niño-3 to define the ENSO phases of the reference summer and exclude 1983 and 1997 from our analysis.

3. Seasonal Indo-Pacific SST anomalies

a. El Niño case

Seeking an explanation for the occurrence of normal and above-normal ISMR during El Niño–3m, we compare two composites of seasonal Indo-Pacific SST anomalies (Figs. 1a,b), one derived from normal and above-normal (the middle and highest terciles) ISMR years during El Niño–3m excluding the two outliers that we have mentioned, 1983 and 1997 (hereafter we call these 12 yr "case A"), and the other derived from the larger ensemble of below-normal (the lowest tercile) ISMR years during El Niño–3m (hereafter we call these 25 yr "case B"). Individual years corresponding to cases A and B are listed in Table 1. The year 1983 has the warmth of the long-lasting, very strong 1982/83 period in the boreal winter and strengthens the mean El Niño warming in the boreal winter in case A. Thus, it is more appropriate to discuss without this outlier whether noncanonical, early El Niño development is linked to ISMR variability. On the other hand, 1997 shows strong El Niño warming during the summer monsoon season and enhances the mean strength of the summer monsoon El Niños in case A, thus to argue whether the ISMR is associated with not the strength of ENSO of the summer monsoon season but the timing of ENSO development, it is more appropriate to exclude the year 1997 from case A. Therefore, we take the conservative way and exclude 1983 and 1997, which favor our argument; however, the results do not differ substantially when these years are included in case A (see the appendix).

In Fig. 1 the seasonal mean Indo-Pacific SST anomalies for case A and case B patterns display a striking difference in seasonal Indo-Pacific SST evolutions. In case A (Fig. 1a), warming over the central-eastern equatorial Pacific, near the date line, and the Niño-1.2 region has already started in December–January–February (DJF), two seasons preceding the reference summer monsoon season. In case B (Fig. 1b), warming over the eastern equatorial Pacific appears in March–April–May (MAM), the time when the typical El Niño cycle starts. In case A warming over the northern Indian Ocean basin and southern Indian Ocean near Madagascar that might be related to the Pacific events (Wang et al. 2003) is prominent in both MAM and June–July–August (JJA) but not so in case B. The horseshoe-shaped cooling over the western Pacific is weak in case A during JJA. These SST patterns are consistent with other variables. In case A, high pressure over the Maritime Continent appear in the boreal winter but not in case B. Particularly during JJA over the equatorial Indian Ocean, negative zonal wind anomalies corresponding to the mean sea level pressure (Kaplan et al. 2000) gradient between the Maritime Continent and the equatorial central Indian Ocean are significantly observed in case A but not in case B (not shown here). However, compared to the SST, the data

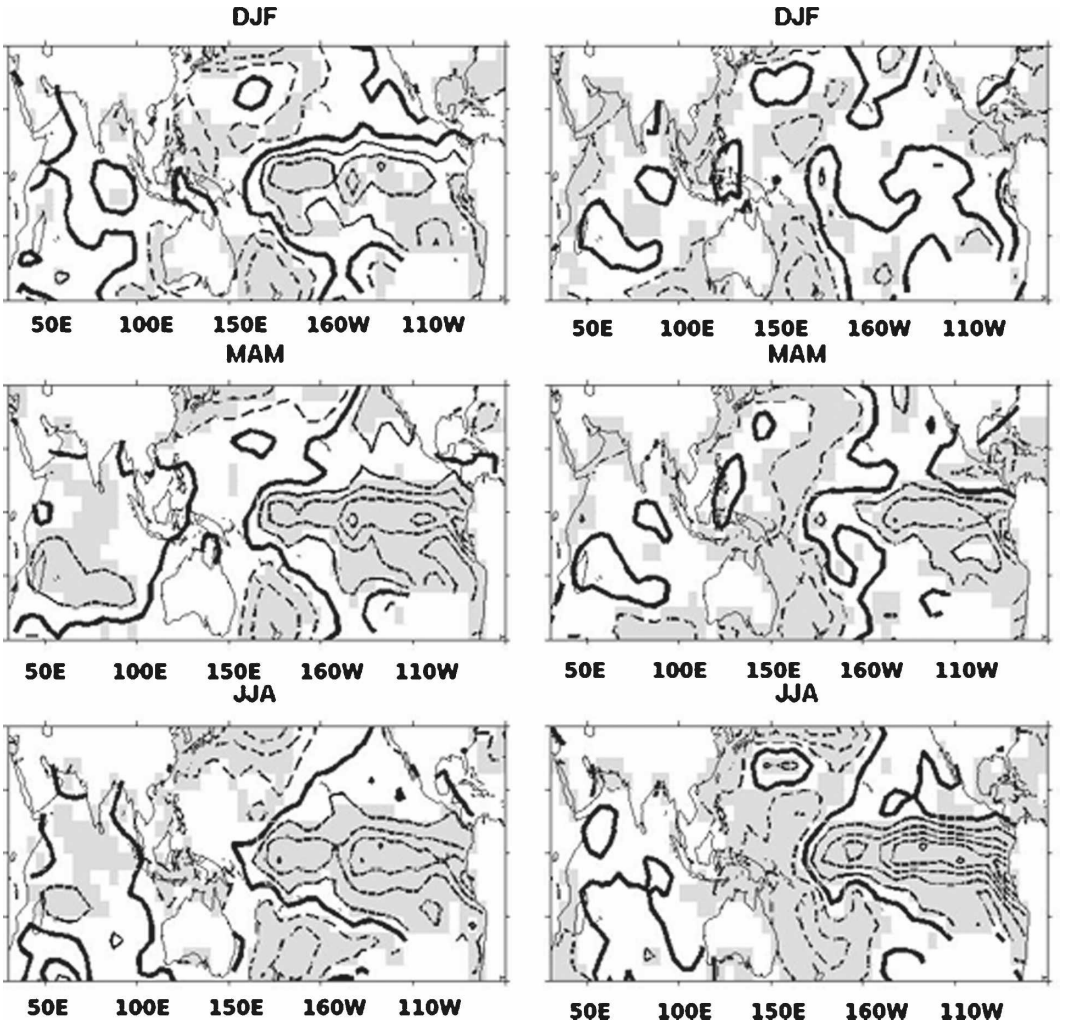

FIG. 1. Seasonal Indo-Pacific SST anomalies in (top) DJF, (middle) MAM, and (bottom) JJA for (left) case A, including years with normal and above-normal ISMR during El Niño–3m except for two outliers, 1983 and 1997, and (right) case B, including years with below-normal ISMR during El Niño–3m. Solid contour lines correspond to positive values and dashed contour lines denote negative values. Thick contour lines indicate 0°C. Contour intervals are 0.2°C. Points that are significantly different from zero means at 90% level and higher using the two-tailed Student's *t* test are shaded.

coverage of sea level pressures before the 1940s is poor (Kaplan et al. 2000), hence the quality of their analysis is less reliable.

Figure 2 shows the composites of mean SST anomalies in case A minus those in case B. The regions where the difference of mean SST anomalies between cases A and B is significant at the 90% level and higher are shaded.[1] Significant warming in the equatorial Pacific from 180° to 140°W and from 90° to 80°W in case A compared to case B is already prominent in DJF (Fig. 2a). In MAM (Fig. 2b), the southern Indian Ocean, the Arabian Sea, and the western-central Pacific from 160°E to 170°W and the South Pacific convergence zone, are significantly warmer in case A than in case B. In JJA (Fig. 2c), over the tropical Pacific Ocean, there is no significant signal over the eastern equatorial Pacific El Niño index regions, but the western-central Pacific from 150° to 175°E at the equator and the South Pacific convergence zone are significantly warmer in case A than in case B. Figure 2c also shows a significant JJA warming in the northern-central Indian Ocean in case A compared to case B, a region that does not show a significant link with ISMR in the usual regression analysis performed for all years. Since

[1] The significance is assessed using a two-sample, two-tailed, Student's *t* test.

TABLE 1. List of individual years corresponding to cases A and B.

Case A	Case B
1884	1888
1896	1891
1900	1899
1914	1902
1919	1904
1926	1905
1940	1911
1953	1913
1963	1915
1969	1918
1976	1920
1993	1923
	1925
	1929
	1930
	1941
	1951
	1957
	1965
	1968
	1972
	1979
	1982
	1987
	1991

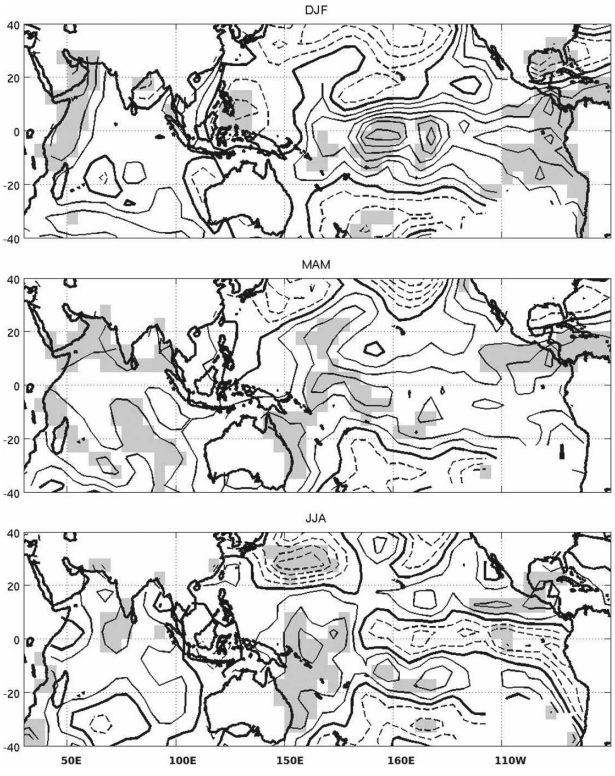

FIG. 2. Composites of the mean Indo-Pacific SST anomalies in case A minus those in case B. Cases are the same as defined in Fig. 1. The regions where the difference of mean SST anomalies between cases A and B is significant at 90% and higher are shaded: (top) DJF, (middle) MAM, and (bottom) JJA. Solid contour lines correspond to positive values and dashed contour lines denote negative values. Thick contour lines indicate 0°C. Contour intervals are 0.1°C.

the Indian Ocean displays a clear warming trend particularly in recent decades, we repeated the same analysis removing a linear trend from the Indian Ocean SST and found little effect on our results. These results imply that the normal and above-normal ISMR during El Niño–3m may be associated with an early development of El Niño in boreal winter and consequently with warmer western-central Pacific and northern-central Indian Ocean SST in boreal summer in case A than in case B.

Measuring the El Niño of the reference summer by using Niño-3.4 does not impact our results; again there is earlier El Niño development in case A (including 1997 since it is not an outlier) than case B. Significance over the northern-central Indian Ocean and western-central Pacific is independent of which ENSO index is used.

The association between a wet monsoon during El Niño–3m and the atypical El Niño evolution found using the Kaplan SST dataset is also confirmed using the Hadley Centre sea ice and SST dataset (HadISST; Rayner et al. 2003; see the appendix in the current paper). However, the warming over the equatorial western-central Pacific is significant only south of the equator in the HadISST dataset. The northern-central Indian Ocean that is significant in JJA in the Kaplan SST is not significant at the 90% level in the HadISST. Sensitivities to the datasets of the significance level differences in SST in the tropical Indo-Pacific Oceans are summarized in the appendix. The differences of significance over these regions may result from the small-scale variability captured in the HadISST but not in the Kaplan SST. The main objective of our study is to investigate the broadscale SST patterns that are associated with normal and above-normal ISMR during El Niño–3m, so the Kaplan SST may be more appropriate.

b. La Niña case

For La Niña cases, we examine the composites of mean SST anomaly difference between case C, including all La Niña–3m years when ISMR falls in the highest tercile of the distribution and case D, including all La Niña–3m years when ISMR falls in the lowest or middle tercile of the distribution. Unlike El Niño–3m years, during La Niña–3m, there is no significant SST anomaly difference between cases C and D over the

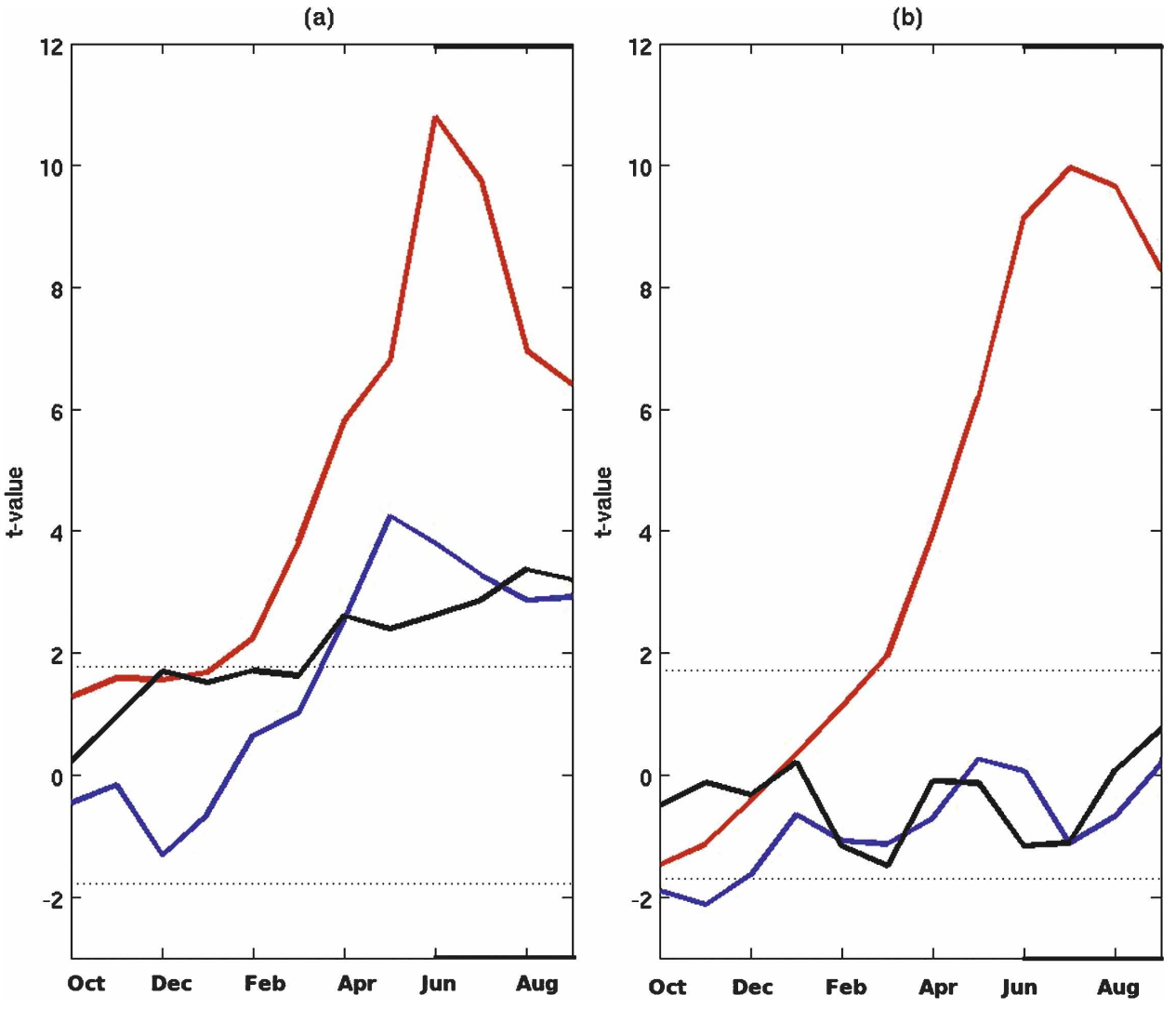

FIG. 3. Composite means of monthly Niño-3, WCP, and NCI from the previous October to the following September, the end of the reference summer monsoon season: (a) case A and (b) case B. The *t* values (see text for the calculation) are plotted. The red lines indicate Niño-3, the black lines denote WCP, and the blue lines denote NCI. The horizontal dotted lines indicates the level where the mean is significantly different from a null hypothesis of a mean equaling zero at 90%.

equatorial Pacific during either DJF or MAM. The colder SST over the eastern equatorial Pacific persists more strongly into the monsoon season in cases C than in D. Thus, we infer that during La Niña–3m, ISMR values are associated with the intensity of Pacific events during the monsoon season rather than the timing of the onset of the cooling. The same results are obtained with La Niña–3.4m.

4. Monthly evolutions of Indo-Pacific SST indices

It appears that the association between ISMR and the timing of ENSO development and ENSO-related anomalies is relevant only in the warm ENSO phase and we further examine this association using indices that are obtained from the Indo-Pacific SST anomalies. Based on the previous composite maps, monthly SST anomalies are averaged over the western-central Pacific (WCP) between 0°–10°S and 160°–175°E and the northern-central Indian Ocean (NCI) between 5°N–10°S and 65°–85°E. We remove the warming trend from NCI using a linear best-fit line over the entire period, although not removing it does not substantially change the results. We do not remove the trend from WCP since most of the warming trend there occurs at the end of the period analyzed, beginning in the 1980s. Figure 3 presents composite mean monthly Niño-3, WCP and

NCI from the previous October to the following September, the end of the reference summer monsoon season; (Fig. 3a) for case A and (Fig. 3b) for case B. Cases A and B are defined as before. The t values are plotted.[2] The horizontal lines indicate the 90% level where the signal is significantly different from a null hypothesis of a mean equaling zero.

In case A (Fig. 3a), the significant warming appears in the Niño-3 region in February. Warming increases slowly toward the reference summer, peaks in the early summer monsoon season, and weakens at the end of the summer monsoon season. In case B (Fig. 3b), Niño-3 is not significantly warmer than usual until March. Warming develops rapidly toward the reference summer. Note that in both cases A and B the composite means of Niño-3 values do not decay after the summer monsoon season. Figure 3 exaggerates the Niño-3 values of the reference summer since t values are plotted and the standard deviations are small during the summer monsoon months. As mentioned above, the basinwide Indian Ocean SSTs are warmer than normal approximately 3–6 months after the occurrence of El Niño events. This lagged relationship between the Indian Ocean SST and Pacific events is consistent with these composites. In case A, ENSO indices begin to warm in boreal winter so that NCI is significantly warmer than usual from April, whereas in case B, the El Niño–related warming over the NCI region misses the summer monsoon season and appears only in the boreal fall. El Niño warming extends farther westward in case A prior to and during the summer monsoon season as indicated by WCP being significantly warmer than usual in the boreal spring and summer, while in case B significant warming over WCP appears after the summer monsoon season. The earlier occurrence of El Niño in case A is also confirmed with different measures of ENSO: the Darwin sea level pressure (DSLP), Niño-1.2 (SST anomalies averaged between 0°–10°S and 80°–90°W) and Niño-4 (SST anomalies averaged between 5°N–5°S and 150°E–160°W). In case A, the significant warming appears in the Niño-1.2 region in December, but in case B, Niño-1.2 is not significantly warmer than usual until February. Niño-4 is warmer than normal in case A in February, but not prior to the summer monsoon season in case B.

Figure 4 shows the difference of mean indices between cases A and B from the previous October to the following September. Asterisks denotes the month where the difference in mean SST anomalies between cases A and B are significant at the 90% level and higher according to a two sample Student's t test. Niño-3 does not show a significant difference during the reference summer monsoon season, JAS, nor do Niño-1.2, Niño-4, or DSLP. Thus, again it is confirmed that the strength of El Niño during the summer monsoon season is not related to normal and above-normal ISMR during El Niño events. WCP and NCI are significantly warmer in case A than in case B during April and throughout the summer monsoon season.

5. Summary and discussion

From our statistical analysis of the observational datasets, we conclude that during the period analyzed, from the late nineteenth century throughout the twentieth century, when ISMR values fall in the middle and upper terciles despite having June–September Niño-3 values in the upper tercile, warming over the eastern equatorial Pacific tends to start about two seasons prior to the reference summer monsoon season. It is associated with warmer than usual WCP and NCI during spring and continuing through the summer monsoon season. Whereas, when ISMR is in the lower tercile of the distribution during the years having June–September Niño-3 values in the upper tercile, warming in the eastern equatorial Pacific tends to develop rapidly from one season ahead of the reference summer monsoon season so that the WCP and NCI are colder during the summer monsoon season than when ISMR is in the middle and upper terciles. These results are statistically not sensitive to including either, 1983, the rapidly decaying El Niño year or 1997, the extremely strong El Niño year, or both of these outliers.

The causality of the associations suggested above is not clear from our statistical work. There have been some modeling studies investigated the physical mechanisms through which the Indo-Pacific SST anomalies impacted the ENSO–monsoon relationship (Wu and Kirtman 2004; Krishna Kumar et al. 2006). Krishna Kumar et al. (2006), using an atmospheric general circulation model with idealized strong El Niño warming, found that the link between El Niño and poor Indian summer monsoon was stronger when the El Niño warming in the eastern Pacific Ocean extended westward to the Niño-4 region compared to when it was confined to a region farther to the east. Our study does not demonstrate a significant difference of Niño-4 and Niño-1.2 regions in either cases A or B during the summer monsoon season. Rather, El Niño–induced warming during the summer monsoon season in the NCI and WCP are significantly different between these cases

[2] The t value is defined as $\mu/(s^2/n)^{1/2}$, where μ is the mean, s is the monthly standard deviation of the composite members, and n is the number of the composite members. A two-tailed test is applied.

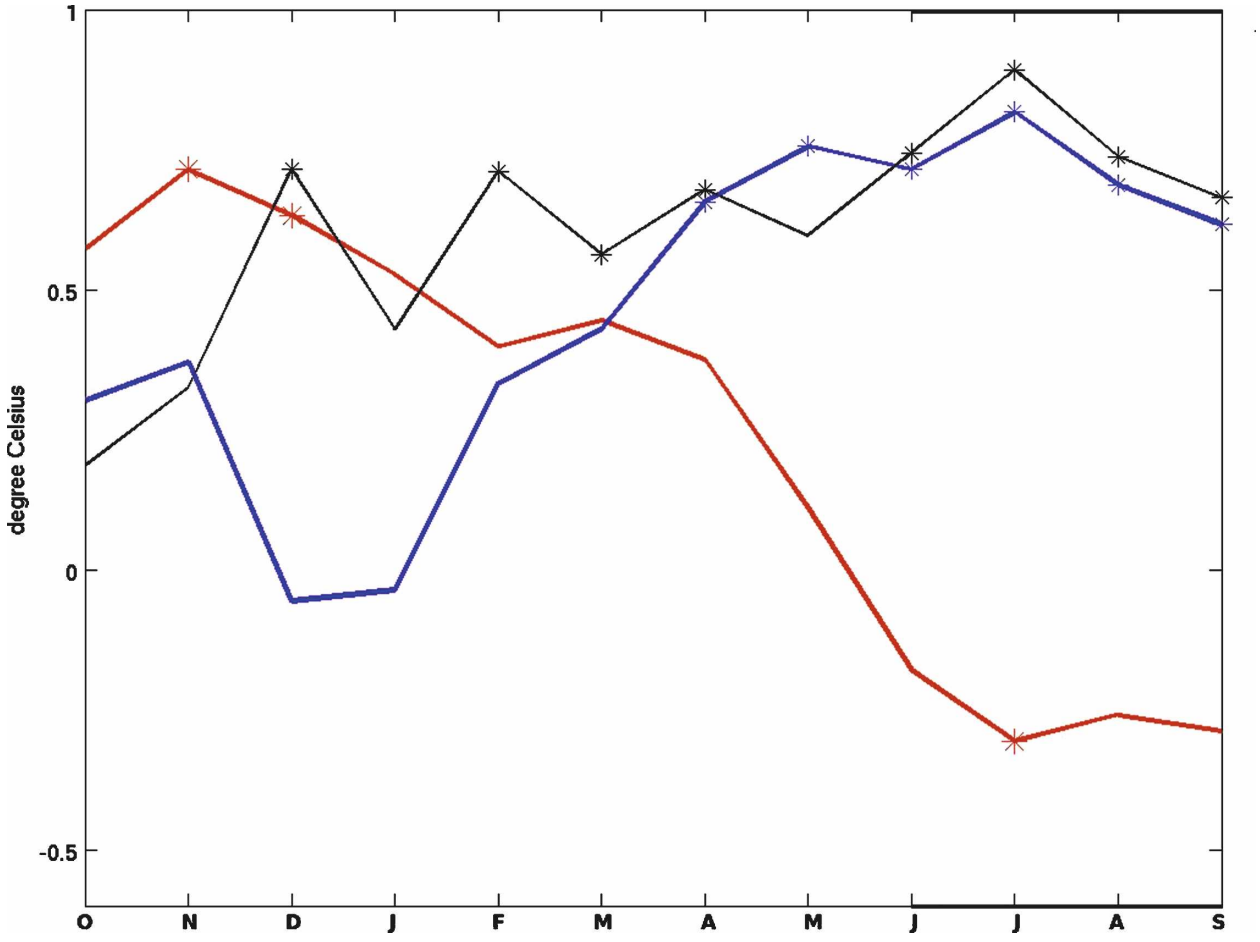

FIG. 4. The difference of mean monthly Niño-3, WCP, and NCI between cases A and B, from the previous October to the following September, the end of the reference summer monsoon season. The red line indicates Niño-3, the black line indicates WCP, and the blue line indicates NCI. Asterisks denote the months where the difference is significant at 90% level and higher using the two-sample Student's *t* test.

(Fig. 2c). It would be interesting to compare the precipitation over India in the general circulation models forced with canonically evolving SST anomalies over the Pacific Ocean to the precipitation in the models forced with noncanonically evolving Pacific SST anomalies that are one season ahead of or behind the canonical evolution.

We propose two hypotheses regarding the physical mechanisms of the three-way associations between the timing of El Niño evolutions, SSTs over the northern-central Indian Ocean and western-central Pacific, and ISMR variability. (i) The state of the western Pacific plays an important role for ISMR variability. During an El Niño event when WCP is warmer than usual in boreal summer, the western Pacific, around 120°–140°E, is not as cold as it is during the canonical El Niño events and the El Niño–induced change over the western Pacific may be weaker. Thus, it can be speculated that the reduction of the condensational heating during El Niños that is thought to suppress the convection over India (Lau and Nath 2000) is weaker or misses India during such cases. (ii) The Indian Ocean SSTs are passively responding to Pacific events. But an early development of El Niño brings about changes in atmospheric thermodynamic stability over the Indian Ocean during the summer monsoon season. During El Niño events, the tropospheric temperature is warmer than usual (Yulaeva and Wallace 1994) but the ocean remains cold because of the larger oceanic thermal inertia; thus, the atmosphere over the ocean is stable (Chiang and Sobel 2002). However, when an El Niño develops from boreal winter, the Indian Ocean is warm during the summer monsoon season, so the atmosphere over the Indian Ocean is less stable. Thus, convection can develop over the western part of the northern Indian Ocean and may lead to increased precipitation over India (Gadgil et al.

2003). The increased rainfall over the Indian Ocean and India when the Indian Ocean was warmer than normal was also demonstrated by Yang et al. (2007).

There are other factors that are known to influence ISMR variability (Webster et al. 1998) besides the Indian and Pacific Ocean SSTs, such as the land conditions over the Indian monsoon region represented by the surface temperature and soil moisture. The protracted warming over the equatorial Pacific from boreal winter throughout the summer monsoon season and the continuing forcing from the Pacific Ocean for several seasons may impact these factors and change the strength of the Indian summer monsoon.

The breakdown of the El Niño–monsoon relationship occurs frequently after the 1980s. For example, the year 1997 had the strongest El Niño of the twentieth century, but the El Niño started rising rapidly in spring to a very large warming while ISMR was normal. The weak rapid rise in the El Niño of 2002 is associated with severe drought, but only in July. Our thesis regarding the association between ISMR variability and the timing of El Niño–related warming does not completely explain the extreme features of individual events, but it does propose robust features of Indo-Pacific SST evolution associated with the wet monsoon during El Niño events of the summer monsoon season starting in the late nineteenth century and lasting through most of the twentieth century.

Acknowledgments. We thank Dr. Sulochana Gadgil for helpful comments. This work was supported under the Cooperative Institute for Climate Applications and Research (CICAR) Award NA03OAR4320179 from the National Oceanic and Atmospheric Administration–Department of Commerce. CI was supported by NASA under the Earth System Science Fellowship Grant NGT5. YK and MAC were supported under NSF Grant ATM0347009. AK was supported by NSF Grants ATM02-33651 and ATM04-17909.

APPENDIX

Sensitivity of Significance to Datasets and Categorizations

Significance levels of the tropical Indo-Pacific SST anomaly difference between two cases based on the Kaplan SST and HadISST are summarized in the table below. The mean SST anomalies over the ENSO, NCI, and WCP regions when ISMR is normal or above normal during El Niños of the monsoon season is compared to the means when ISMR is below normal during El Niños of the monsoon season. Sensitivity of excluding both of the extreme years, 1983 and 1997, or either of them from the years when ISMR is normal or above normal during the El Niño of the monsoon season (case A) to significance levels is presented. Bold font shows the category that is analyzed in this paper. Significance is assessed by two-sample, two-tailed Student's *t* test.

		ENSO region	NCI region	WCP region
Kaplan	Include all years	90%	90%	90%
	Exclude 1997 and 1983	**90%**	**90%**	**90%**
	Exclude 1997	90%	90%	90%
	Exclude 1983	90%	90%	90%
HadISST	Include all years	90%	90%	80%
	Exclude 1997 and 1983	90%	Not significant	80%
	Exclude 1997	90%	90%	90%
	Exclude 1983	90%	80%	90%

REFERENCES

Alexander, M. A., I. Blade, M. Newman, J. R. Lanzante, N. C. Lau, and J. D. Scott, 2002: The atmospheric bridge: The influence of ENSO teleconnections on air–sea interaction over the global oceans. *J. Climate,* **15,** 2205–2231.

Ashok, K., Z. Guan, N. H. Saji, and T. Yamagata, 2004: Individual and combined influences of the ENSO and the Indian Ocean dipole on the Indian summer monsoon. *J. Climate,* **17,** 3141–3154.

——, S. K. Behera, S. A. Rao, H. Weng, and T. Yamagata, 2007: El Niño Modoki and its possible teleconnection. *J. Geophys. Res.,* **112,** C11007, doi:10.1029/2006JC003798.

Chiang, J. C. H., and A. H. Sobel, 2002: Tropical tropospheric temperature variations caused by ENSO and their influence on the remote tropical climate. *J. Climate,* **15,** 2616–2631.

Gadgil, S., P. N. Vinayachandran, and P. A. Francis, 2003: Droughts of the Indian summer monsoon: Role of clouds over the Indian Ocean. *Curr. Sci.,* **85** (12), 1713–1719.

Kaplan, A., M. Cane, Y. Kushnir, A. Clement, M. Blumenthal, and B. Rajagopalan, 1998: Analyses of global sea surface temperature 1856-1991. *J. Geophys. Res.,* **103,** 18 567–18 589.

——, Y. Kushnir, and M. A. Cane, 2000: Reduced space optimal interpolation of historical marine sea level pressure. *J. Climate,* **13,** 2987–3002.

——, M. A. Cane, and Y. Kushnir, 2003: Reduced space approach to the optimal analysis interpolation of historical marine observations: Accomplishments, difficulties, and prospects. *Advances in the applications of marine climatology: The dynamic part of the WMO guide to the applications of marine climatology,* WMO/TD-1081, World Meteorological Organization, 199–216.

Krishna Kumar, K., B. Rajagopalan, M. Hoerling, G. Bates, and M. A. Cane, 2006: Unraveling the mystery of Indian monsoon failure during El Niño. *Science,* **314,** 115–119.

Lau, N.-C., and M. J. Nath, 2000: Impact ENSO on the variability of the Asian–Australian monsoons as simulated in GCM experiments. *J. Climate,* **13,** 4287–4309.

Rasmusson, E. M., and T. H. Carpenter, 1982: Variations in tropical sea surface temperature and surface wind fields associated

with the Southern Oscillation/El Niño. *Mon. Wea. Rev.,* **110,** 354–384.

——, and ——, 1983: The relationship between eastern equatorial Pacific sea surface temperatures and rainfall over India and Sri Lanka. *Mon. Wea. Rev.,* **111,** 517–528.

Rayner, N. A., D. E. Parker, E. B. Horton, C. K. Folland, L. V. Alexander, D. P. Rowell, E. C. Kent, and A. Kaplan, 2003: Global analyses of sea surface temperature, sea ice, and night marine air temperature since the late nineteenth century. *J. Geophys. Res.,* **108,** 4407, doi:10.1029/2002JD002670.

Ropelewski, C. F., and M. S. Halpert, 1987: Global and regional scale precipitation patterns associated with the El Niño/Southern Oscillation. *Mon. Wea. Rev.,* **115,** 1606–1626.

Sontakke, N. A., G. B. Pant, and N. Singh, 1993: Construction of all-India summer monsoon rainfall series for the period 1844–1991. *J. Climate,* **6,** 1807–1811.

Wang, B., R. Wu, and T. Li, 2003: Atmosphere–warm ocean interaction and its impacts on Asia–Australian monsoon variation. *J. Climate,* **16,** 1195–1211.

Webster, P. J., V. O. Magana, T. N. Palmer, J. Shukla, R. A. Tomas, M. Yanai, and T. Yasunari, 1998: Monsoon: Processes, predictability and the prospects for prediction. *J. Geophys. Res.,* **103** (C7), 14 451–14 510.

Weng, H., K. Ashok, S. K. Behera, S. A. Rao, and T. Yamagata, 2007: Impacts of recent El Niño Modoki on dry/wet conditions in the Pacific rim during boreal summer. *Climate Dyn.,* **29,** 113–129.

Wu, R., and B. P. Kirtman, 2004: Impact of the Indian Ocean on the Indian Summer Monsoon–ENSO relationship. *J. Climate,* **17,** 3037–3054.

Yang, J., Q. Liu, S. P. Xie, Z. Liu, and L. Wu, 2007: Impact of the Indian Ocean SST basin mode on the Asian summer monsoon. *Geophys. Res. Lett.,* **34,** L02708, doi:10.1029/2006GL028571.

Yulaeva, E., and J. M. Wallace, 1994: The signature of ENSO in global temperature and precipitation fields derived from the microwave sounding unit. *J. Climate,* **7,** 1719–1736.